Modulating Oral Delivery and Gastrointestinal Kinetics of Recombinant Proteins via Engineered Fungi

Mairead K. Heavey[1] and Aaron C. Anselmo[1,2]

Received 1 March 2021; accepted 30 April 2021; published online 19 May 2021

Abstract. A new modality in microbe-mediated drug delivery has recently emerged wherein genetically engineered microbes are used to locally deliver recombinant therapeutic proteins to the gastrointestinal tract. These engineered microbes are often referred to as live biotherapeutic products (LBPs). Despite advanced genetic engineering and recombinant protein expression approaches, little is known on how to control the spatiotemporal dynamics of LBPs and their secreted therapeutics within the gastrointestinal tract. To date, the fundamental pharmacokinetic analyses for microbe-mediated drug delivery systems have not been described. Here, we explore the pharmacokinetics of an engineered, model protein-secreting *Saccharomyces cerevisiae*, which serves as an ideal organism for the oral delivery of complex, post-translationally modified proteins. We establish three methods to modulate the pharmacokinetics of an engineered, recombinant protein-secreting fungi system: (i) altering oral dose of engineered fungi, (ii) co-administering antibiotics, and (iii) altering recombinant protein secretion titer. Our findings establish the fundamental pharmacokinetics which will be essential in controlling downstream therapeutic response for this new delivery modality.

KEY WORDS: engineered fungi; live biotherapeutic products; oral delivery; pharmacokinetics; recombinant proteins.

INTRODUCTION

The community of bacteria and fungi in the human gastrointestinal (GI) tract has been shown to play crucial roles in human health (1), immunity (2), and disease progression (3). Past research efforts in the GI microbiome space have been focused on addressing questions related to what microbes are present in the GI tract (4–7), what functions they are performing (8–10), and how these functions relate to the initiation or progression of a specific disease (11–13). As the various roles of the microbiome in health and disease have been described, the development and oral delivery of live biotherapeutic products (LBPs) has emerged as a strategy to elicit novel functions in the GI tract (14–16) (e.g., metabolism of indigestible or toxic compounds (17), diagnosis of disease pathologies (18), local delivery of drugs or biologics (19–21)). Oral administration is considered the most convenient route of administration; however, oral delivery of biologics remains a challenge due to the harsh environment of the early GI tract (22) and biological barriers that limit absorption (23). LBPs can potentially enable the local delivery of biologics via the oral route by (i) circumventing harsh environments in the early GI tract, (ii) proliferating and persisting in the GI tract, and (iii) secreting recombinant proteins directly in the small and large intestines (colon). While over 15 genetically engineered LBPs are currently being evaluated in clinical trials via oral delivery (24,25), much is unknown about their pharmacokinetics and thus how to optimize and control their therapeutic benefit.

As the oral delivery of LBPs emerges as a strategy for local GI delivery of recombinant therapeutics, a critical analysis of the pharmacokinetics is essential. Pharmacokinetic analyses of other therapeutic modalities (e.g., small molecules, antibodies, peptides) have allowed us to understand drug biodistribution, develop methods to control drug concentrations at specific times/physiological locations, predict the total drug exposure under various disease states and conditions, and accurately scale up distribution data from small animals up to humans (26–28). However, the fundamental analyses of microbe and secreted protein GI kinetics have not been previously investigated or described. This

Guest Editors: Aliasger Salem, Juliane Nguyen and Kristy Ainslie

[1] Division of Pharmacoengineering and Molecular Pharmaceutics, Eshelman School of Pharmacy, University of North Carolina at Chapel Hill, 125 Mason Farm Road, North Carolina 27599, Chapel Hill, USA.

[2] To whom correspondence should be addressed. (e–mail: aanselmo@email.unc.edu)

current knowledge gap may be due to the unique challenges that separate LBPs from other therapeutic modalities such as *in vivo* proliferation, lack of established approaches for measuring dynamic local drug concentrations in the GI tract (unlike serum measurements), and the limited knowledge as to how native members of the microbiome influence LBP pharmacokinetics (29–31). Identifying and describing key factors that influence the local concentrations of the LBP and its secreted proteins in specific physiologic locations throughout the GI tract may eventually enable delivery of a controlled dose of therapeutics from the LBP. For example, the treatment of ulcerative colitis with punctate sites of inflammation (32) or in colorectal cancer where there exist specific tumor sites in the GI tract (33) could benefit from control over local therapeutic concentration.

Here, we aim to establish approaches to characterize and modulate the *in vivo* GI pharmacokinetics of an engineered, recombinant protein-secreting fungi; in doing so, we describe the fundamental pharmacokinetics of the living microbe and its secreted recombinant protein for the first time. First, we engineered *Saccharomyces cerevisiae* to secrete green fluorescent protein (GFP) to serve as a model LBP for the oral delivery of biologics. *S. cerevisiae* is an ideal model organism because it can secrete high titers of recombinant proteins with eukaryotic post-translational modifications (34), survive and maintain metabolic activity in both aerobic and anaerobic environments that exist throughout the GI tract (35,36), and serve as a safe genetically engineered microbial chassis for delivery to humans, since it is unlikely to initiate horizontal gene transfer to the microbes native to the GI tract (37,38). GFP serves as an ideal model biologic because it is a well-characterized, complex protein which requires post-translational modifications, it allows for straightforward quantification from feces/tissues, and it has been previously optimized for secretion by *S. cerevisiae* (39). Using this model system, we establish three distinct and tunable delivery strategies to modulate the *in vivo* pharmacokinetics of both the engineered fungi and the secreted biologic: (i) altering oral dose of engineered fungi, (ii) co-administering antibiotics, and (iii) altering recombinant protein secretion titer. Briefly, we found that initial dose influenced local recombinant protein concentrations in the GI tract as soon as 12 h post-administration, the co-administration of antibiotics influenced the persistence of both the engineered fungi and secreted GFP within the GI tract, and the *in vitro* recombinant protein secretion titer influenced *in vivo* local concentrations of the protein within the GI tract. Our results define important considerations for the oral delivery of various protein and peptide pharmaceuticals to the GI tract via LBPs.

MATERIALS AND METHODS

Strains and Culture Media

Escherichia coli Top10 were used for plasmid amplification and maintenance. *E. coli* was grown in lysogeny broth (LB) containing 5g L^{-1} yeast extract, 10 g L^{-1} tryptone, and 10 g L^{-1} NaCl at 37°C supplemented with ampicillin (100 μg mL^{-1}). *Saccharomyces cerevisiae* strains were derivatives of the haploid strain JK9-3dα, provided by the Heitman lab (40). *S. cerevisiae* was grown at 30°C in rich glucose medium (YPD) containing 10 g L^{-1} yeast nitrogen base, 20 g L^{-1} peptone, and 20 g L^{-1} D-(+)-glucose and supplemented with 20 mg L^{-1} of adenine and uracil. Positive transformants were grown and selected for on minimal glucose dropout medium (SD-CAA) (41) containing 20 g L^{-1} dextrose, 6.7 g L^{-1} Difco yeast nitrogen base, 5 g L^{-1} Bacto casamino acids, 5.4 g L^{-1} Na_2HPO_4, 8.56 g L^{-1} $NaH_2PO_4{\cdot}H_2O$, and 20 mg L^{-1} of adenine and uracil.

Plasmid Construction and Transformation

The integrative plasmid for secretion of GFP was synthesized as previously described (39) by commercial gene synthesis (Synbio Technologies). The integrative plasmid was linearized with EcoRV (New England Biolabs) to direct genomic integration. Competent fungi were prepared and transformed with linearized DNA as previously described using the LiAc/PEG method (42). Briefly, fungi were inoculated in 50 mL fresh YPD medium to reach an OD_{600} of 1.6 and were then collected via centrifugation. Fungi were washed 3 times with 50 mL sterile water and resuspended with 1 mL sterile water and then separated into 100 μL aliquots. For transformation, 360 μL of "transformation mix" containing PEG 3350 (50% w/v), lithium acetate (1.0 M), single-stranded carrier DNA (2.0 mg mL^{-1}), and the linearized plasmid DNA was added to the prepared aliquot of competent fungi. This mixture was incubated in a water bath at 42°C for 40 min. Transformed fungi were then collected via centrifugation, resuspended in sterile water, and plated on selective SD-CAA agar plates lacking tryptophan. Plates were incubated for 3 days at 30°C. Positive transformants were confirmed via fluorescence microscopy, and transformants were screened for differential GFP expression by ELISA.

Detection and Quantification of GFP

For western blot detection of secreted GFP, each of the isolates was grown overnight in 5 mL YPD at 37°C under both aerobic and anaerobic conditions. Cultures were centrifuged at 3000 rpm for 3 min, and supernatants were collected. Proteins in the culture supernatant were precipitated by acetone. Protein precipitates were then treated with EndoH (New England Biolabs) enzyme to remove excess glycosylation to prevent band smearing. Samples were then subject to standard gel electrophoresis sample preparation, loaded onto a 4–20% Mini-PROTEAN® TGX™ precast gel (BioRad), and ran with standard gel electrophoresis parameters. Proteins were transferred from the gel to a nitrocellulose membrane overnight at 4°C using a constant 30 mA in the blotting module. The membrane was washed with sterile water, blocked with 1% Pierce™ Clear Milk Blocking Buffer (Thermo Fisher Scientific), and blotted with 1:5000 dilution of an anti-GFP antibody conjugated to horseradish peroxidase (HRP) (Abcam). To enable band detection, the Pierce ECL Western Blotting Substrate (Thermo Fisher Scientific) was used. The membrane was immediately imaged using a FluorChem E Imager (Protein Simple) using standard chemiluminescence exposure parameters.

To detect secreted GFP in both the *in vitro* culture supernatants and within fecal and tissue samples, an in-house enzyme linked immunosorbent assay (ELISA) was used. Briefly, 1.25 μg mL^{-1} anti-GFP antibody (Abcam) in a sodium bicarbonate buffer at pH 9.4 was incubated on a Nunc MaxiSorp flat-bottom 96-well plate (Thermo Fisher Scientific) overnight at 4°C. The plate was washed 3 times with phosphate buffered saline containing 0.05% Tween 20 (PBST). Then a 1% bovine serum albumin solution in PBS was added to the wells. Wells were blocked at room temperature with gentle shaking for 2 h. The plate was washed 3 times with PBST, and then samples diluted in PBST and a GFP (Abcam) standard curve (250–0.12 ng mL^{-1}) were loaded onto the plate and incubated at room temperature with gentle shaking for 2 h. The plate was then washed 3 times with PBST, and a 1:2500 dilution of an anti-GFP-HRP antibody (Abcam) was loaded onto the plate and incubated at room temperature with gentle shaking for 1 h. The plate was then washed 5 times with PBST, and 1-Step Ultra TMB-ELISA Substrate Solution (Thermo Fisher Scientific) was added for quantification. The enzymatic reaction was stopped with 2M sulfuric acid, and optical density at 450 nm was read using a SpectraMax iD3 96-well plate reader (Molecular Devices). Each biological replicate was analyzed in duplicate technical replicates on the ELISA plates. Final concentrations were determined by using the average optical density values of the two technical replicates.

In Vitro Growth and GFP Secretion Assays

Isolates were grown in culture tubes with 5 mL of YPD medium at either 30°C or 37°C and under either aerobic or anaerobic conditions. For anaerobic samples, YPD was stripped of its oxygen content through incubation in an anaerobic chamber overnight. All cultures were kept shaking at 250 rpm at constant temperature in a shaking incubator for the entirety of the study. To track growth, at each time point indicated, the optical density at 600 nm was measured using a GENESYS 30 spectrophotometer (Thermo Fisher Scientific). Immediately thereafter, 100 μL samples were removed from the culture for downstream analyses and replaced with 100 μL of fresh YPD. The samples at each time point were centrifuged at 3000 rpm for 3 min to separate secreted proteins from the fungi. Supernatants were kept at 4°C for next-day analyses.

For intracellular GFP analysis, fungi were grown in a 6-well transwell plate (Corning) with 3.0 μm membrane insert where fungi suspended in 1 mL YPD were placed atop the membrane and could be exposed to fresh YPD below the membrane. This was to physically separate the fungi from the media for the entirety of the study. Cultures were grown overnight at 37°C with 100 rpm shaking. The membranes were then removed, and the fungi-free media was analyzed by ELISA as described. Fungi on the membrane were collected, washed with PBS, resuspended in digestion buffer, and treated with zymolyase enzyme (Zymo Research) to break the fungal microbe walls and release the intracellular proteins. The enzymatic reaction was carried out at 37°C for 1 h. This solution was then centrifuged at 3000 rpm for 3 min, and supernatants containing the intracellular proteins were diluted and subject to ELISA analysis as described previously.

Mouse Experiments

Animal studies were conducted in accordance with and approved by the Institutional Animal Care and Use Committee (IACUC) of The University of North Carolina at Chapel Hill. Eight-week-old female BALB/c mice housed in groups of 5 were used for all *in vivo* studies. Mice were purchased from Charles River Labs and acclimated for at least 72 h prior to use. One mouse was separated from the third mouse study in the group receiving Sc-GFP-Lo due to unrelated health/behavioral concerns. For studies in which antibiotics were used, the antibiotics were administered *ad lib* through the drinking water. Mice which received only a 3-day pre-treatment of antibiotics were placed back on an automatic watering system for the remainder of the study. The antibiotic water cocktail contained ampicillin (0.5 mg mL^{-1}, Sigma), gentamicin (0.5 mg mL^{-1}, Sigma), metronidazole (0.5 mg mL^{-1} Sigma), neomycin (0.5 mg mL^{-1}, Sigma), vancomycin (0.25 mg mL^{-1}, MP Biomedicals), and sucralose (4 mg mL^{-1}, Sigma) as previously described (43,44). The antibiotic water cocktail was prepared on the same day as administration to mice. For continuous antibiotic treatment, fresh antibiotic water cocktail was newly prepared, filter sterilized, and administered every fourth day of the study to ensure antibiotic stability in water at room temperature. For oral administration, fungi were cultured the day prior in YPD media at 30°C (250 rpm). The following day, the culture was washed three times and suspended in sterile saline. In the fungal dose ranging study, mice were administered either 10^9, 10^8, 10^7, or 10^6 colony forming units (CFU) in 150 μL sterile saline via oral gavage. In the antibiotics ranging study, all mice received 10^9 CFU of Sc-GFP-Hi in 150 μL sterile saline via oral gavage, and in the GFP-secretion ranging study, mice received 10^9 CFU of either Sc-GFP-Hi or Sc-GFP-Lo in 150 μL sterile saline via oral gavage.

Stool and Tissue Sample Processing

At indicated time points, each mouse was individually placed in a sterilized cage and approximately 3–5 fecal pellets were collected from each mouse. Pellets were placed in pre-weighed homogenization tubes containing 1.4 mm ceramic beads. Tubes were weighed again to calculate fecal weight, and sterile phosphate buffered saline (PBS) was added to each tube to reach approximately 100 mg feces per 1 mL PBS. Feces were then homogenized with a FastPrep-24 homogenizer (MP Biomedicals) for 20 s at 4.0 M s^{-1}. Samples were filtered through a cell strainer with a 75 μm pore size to remove solid particulates and to allow for a solution that can be drawn up with a pipette and fungal microbes evenly dispersed. Fecal sample solutions were serially diluted in sterile PBS, and dilutions were plated on SD-CAA agar plates containing ampicillin (2.5 μg mL^{-1}, Sigma), gentamicin (2.5 μg mL^{-1}, Sigma), metronidazole (2.5 μg mL^{-1} Sigma), neomycin (2.5 μg mL^{-1}, Sigma), and vancomycin (1.25 μg mL^{-1}, MP Biomedicals) (43). CFUs were enumerated after incubation for 2–3 days at 30°C. CFUs were confirmed via fluorescence microscopy. Mice were sacrificed either 12 h or 168 h post-gavage, and the intestinal tracts were immediately harvested. Specified sections of the intestinal tracts were placed in pre-weighed homogenization tubes containing

2.4 mm ceramic beads. Tissue sample weight was calculated, and 1mL of sterile PBS was added to each tube. The samples were then homogenized for 20 s at 6.5 M s^{-1} and filtered through a cell strainer with a 75 μm pore size. Samples were serially diluted in PBS, and dilutions were plated on SD-CAA plates containing antibiotics as described. CFUs were enumerated as previously described after 2–3 days incubation at 30°C. Homogenization speeds and times were far below standard fungal microbe lysing protocols (45), and these parameters were optimized to prevent fungi lysing in the fecal and tissue samples (Fig. S1).

Data and Statistical Analysis

The number (n) of individual animals used per group is described in each figure legend. CFU enumeration and GFP quantification in the fecal and tissue samples were normalized to either the fecal or tissue weight of the sample. This data was log-transformed to ensure normal distribution of data to allow for downstream statistical analyses. Limit of detection for GFP concentration analyses via ELISA was determined to be the optical density reading at 450 nm which corresponded to the lowest concentration in the linear portion of the standard curve. For CFU counting, 25 to 250 CFUs were considered in the countable range in a 20 μL plated sample. If no colonies were detected, another 250 μL of the sample was separately plated where again, 25 to 250 CFUs were considered in the countable range. Any CFU counts below this range are still plotted as such but appear below the limit of detection (LOD) line. The LOD is calculated as 25 CFUs in 250 μL. All samples which resulted in no detectable CFU were set to one-half of the LOD value. All statistics and data distribution analysis were performed with Prism (GraphPad). The unpaired two-tailed Student's t-test was used to compare differences between two groups. Ordinary one-way ANOVA with multiple comparisons was used to evaluate experiments containing more than two groups. The upper threshold for statistical significance for all experiments was set at $p < 0.05$.

RESULTS

Generation of GFP-Secreting *Saccharomyces cerevisiae* Strains

To evaluate potential approaches to control the concentrations and subsequent *in vivo* pharmacokinetics of LBPs, a model system was generated. The model system consisted of a *Saccharomyces cerevisiae* strain engineered to secrete green fluorescent protein (GFP). The secretion of GFP allowed for easy and rapid confirmation of positive transformants and rapid tracking of colony isolates *in vivo*. A tryptophan auxotrophic *S. cerevisiae* strain (JK9-3dα) was transformed with a linearized plasmid which contained the sequence for GFP preceded by an optimized secretion signal to direct the recombinant protein outside of the fungi (Fig. 1a) as previously described by Fitzgerald and Glick (39). Expression was placed under the control of a constitutive promoter to ensure constant expression. A yeast integrating plasmid lacking an origin of replication was used to direct genomic integration via homologous recombination. By integrating the plasmid directly into the genome, this avoided the necessity for constant selective pressure to maintain the plasmid inside the engineered fungi, which is ideal for the *in vivo* environment where maintaining a constant external selective pressure would be difficult.

Following transformation, positive colony transformants were isolated on selective media lacking tryptophan. Colonies were isolated and screened for differential GFP expression (Fig. S2). Genomic integration via homologous recombination can often result in multiple in-tandem integrations of the linearized plasmid into the integration site (46,47), ultimately leading to higher or lower expression of the recombinant protein depending on the number of genomic integrations (48). After the initial screening for differential expression of GFP, high- and low-secretor transformants were isolated for further analyses, referred to herein as Sc-GFP-Hi and Sc-GFP-Lo, respectively. Expression of GFP in the isolated strains was visualized via fluorescent microscopy (Fig. 1b) which showed the intracellular accumulation of GFP prior to secretion. This also confirmed proper folding of GFP, as fluorescence can only be visualized with the correct post-translational folding (49).

Growth and Differential GFP Expression Under Various Environmental Conditions

To ensure both adequate growth and GFP secretion under a variety of physiologically relevant conditions in the GI tract, the two isolates were grown in environments of different temperatures and oxygen levels. We first assessed growth (Fig. 2a) and GFP secretion (Fig. 2b) under aerobic conditions at 30°C (Fig. 2ai and bi) which are optimal lab conditions for *S. cerevisiae* growth (35), then under aerobic conditions at 37°C (Fig. 2aii and bii) which is representative of physiological conditions in the small intestine, and finally under anaerobic conditions at 37°C (Fig. 2aiii and biii) which is representative of physiological conditions in the colon (36, 50). Fungi grew to a lower final density when grown at 37°C (Fig. 2aii) as compared to 30°C under aerobic conditions (Fig. 2ai); this was expected and can be attributed to the stressful environment at 37°C which can result in preference for fungal maintenance and metabolism over proliferation (51,52). Under all conditions tested, there were no significant differences in growth profiles between Sc-GFP-Hi and Sc-GFP-Lo (Fig. 2a); however, as expected, the Sc-GFP-Hi consistently showed higher final GFP concentrations in the culture supernatant as compared to Sc-GFP-Lo for all conditions evaluated (Fig. 2b). To exclusively quantify secreted GFP (i.e., not intracellular GFP), all samples were centrifuged before ELISA analysis to separate intracellular GFP from the secreted GFP. For further confirmation, the proteins from overnight cultures were precipitated and analyzed by western blot, which showed a single band around 27kDa (Fig. 2c), corresponding to the molecular weight of GFP (53) and thus confirmed the secretion of GFP under both aerobic and anaerobic conditions. We also quantitatively compared the amount of intracellular GFP to the secreted, extracellular GFP between Sc-GFP-Hi and Sc-GFP-Lo under aerobic conditions at 37°C (Fig. 2d). Sc-GFP-Hi secreted significantly higher GFP in the culture supernatant as compared to Sc-GFP-Lo which was consistent with our previous results. Saturated cultures of both isolate strains

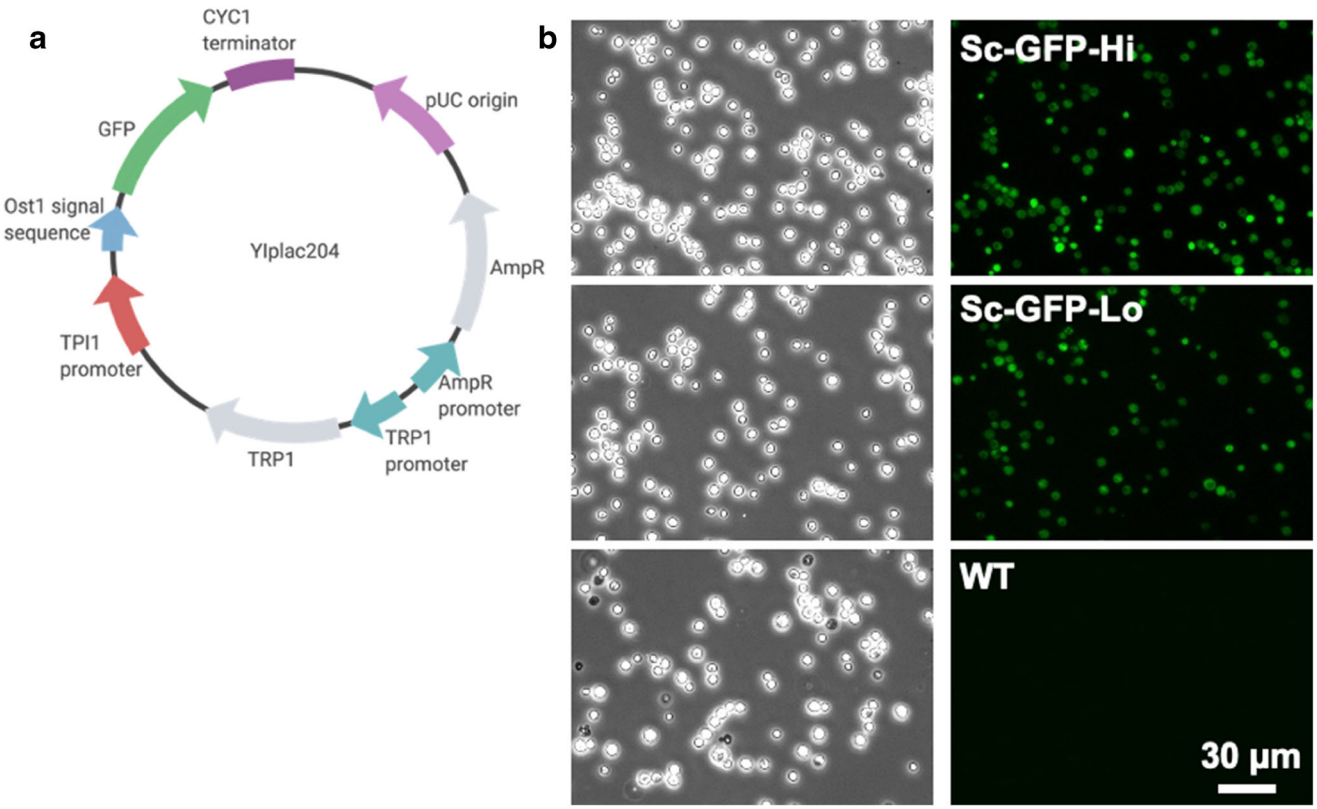

Fig. 1. Engineering *Saccharomyces cerevisiae* to secrete green fluorescent protein. **a** Map of the major components of the integrative plasmid for GFP secretion. **b** Left: Representative differential interference contrast microscope images of wild type and isolated transformants. Right: Representative fluorescence microscope images showing intracellular GFP accumulation in the isolated transformants

showed roughly 95% of the total GFP was extracellular, while intracellular GFP accounted for roughly 5% of the total GFP (Fig. 2e). Taken together, this confirmed that Sc-GFP-Hi produced a greater amount of GFP overall, as opposed to a more efficient GFP secretion.

Approaches to Modulate the *In Vivo* Pharmacokinetics of Engineered Fungi and Secreted GFP

Disposition kinetics of LBPs are rarely studied and reported but are essential to meeting regulatory and safety standards (54,55) and for having a thorough understanding of dose-response relationships *in vivo*. Distinct from other microbes which may colonize and remain at steady-state concentrations in the GI tract, *S. cerevisiae* transiently passes through the GI tract following oral administration (21,56). As such, thorough pharmacokinetic evaluation may identify conditions that can provide desirable dosing regimens. Here, we studied three approaches to modulate the pharmacokinetics of our model system (Fig. 3). These three approaches include modulation by (i) altering oral dose of engineered fungi (Fig. 3a), (ii) co-administration of antibiotics (Fig. 3b), and (iii) altering recombinant protein secretion titer (Fig. 3c).

Influence of Initial Dose on Engineered Fungal and GFP T_{max} Concentrations in Mice

In the first *in vivo* study, we sought to understand how the number of engineered fungi orally delivered affected the local GI concentrations of both the engineered fungi and the secreted GFP at the time of maximal concentration. In a preliminary study, we determined 12 h post-oral gavage to be the time to maximal concentration (T_{max}) of GFP in the feces (Fig. S3). We chose T_{max} to explore the relationship between dose and local concentrations because we hypothesized that this would be the optimal time point to observe maximal differences between groups, given that there is minimal time for non-linear clearance or metabolism processes to confound concentration data.

In this study, mice received a 3-day pre-treatment of a previously described antibiotics cocktail in the drinking water to reduce the overall abundance of endogenous bacteria in the GI tract (43). Growth of the engineered fungi in antibiotics was tested *in vitro* to ensure antibiotic treatment would not inhibit fungal growth *in vivo* (Fig. S4). Mice received either 10^9, 10^8, 10^7, or 10^6 CFU of Sc-GFP-Hi via oral gavage (Fig. 4a). Sc-GFP-Hi colonies isolated from fecal and tissue samples were confirmed via fluorescence microscopy (Fig. 4b). Each 10-fold change in the dose resulted in roughly 10-fold changes in the CFU concentrations in the feces at both 6 and 12 h post-gavage (Fig. 4c). Albeit not as high as 10-fold, GFP concentrations in the feces generally decreased with each decreasing dose (Fig. 4d). This indicated that as soon as 12 h post-gavage, the dose influenced the delivery of the recombinant protein. An analysis of the GI tissues revealed roughly 10-fold decreases in CFU with each 10-fold decrease in dose (Fig. 4e). Significant differences in GFP concentrations were also observed in the GI tissues, with

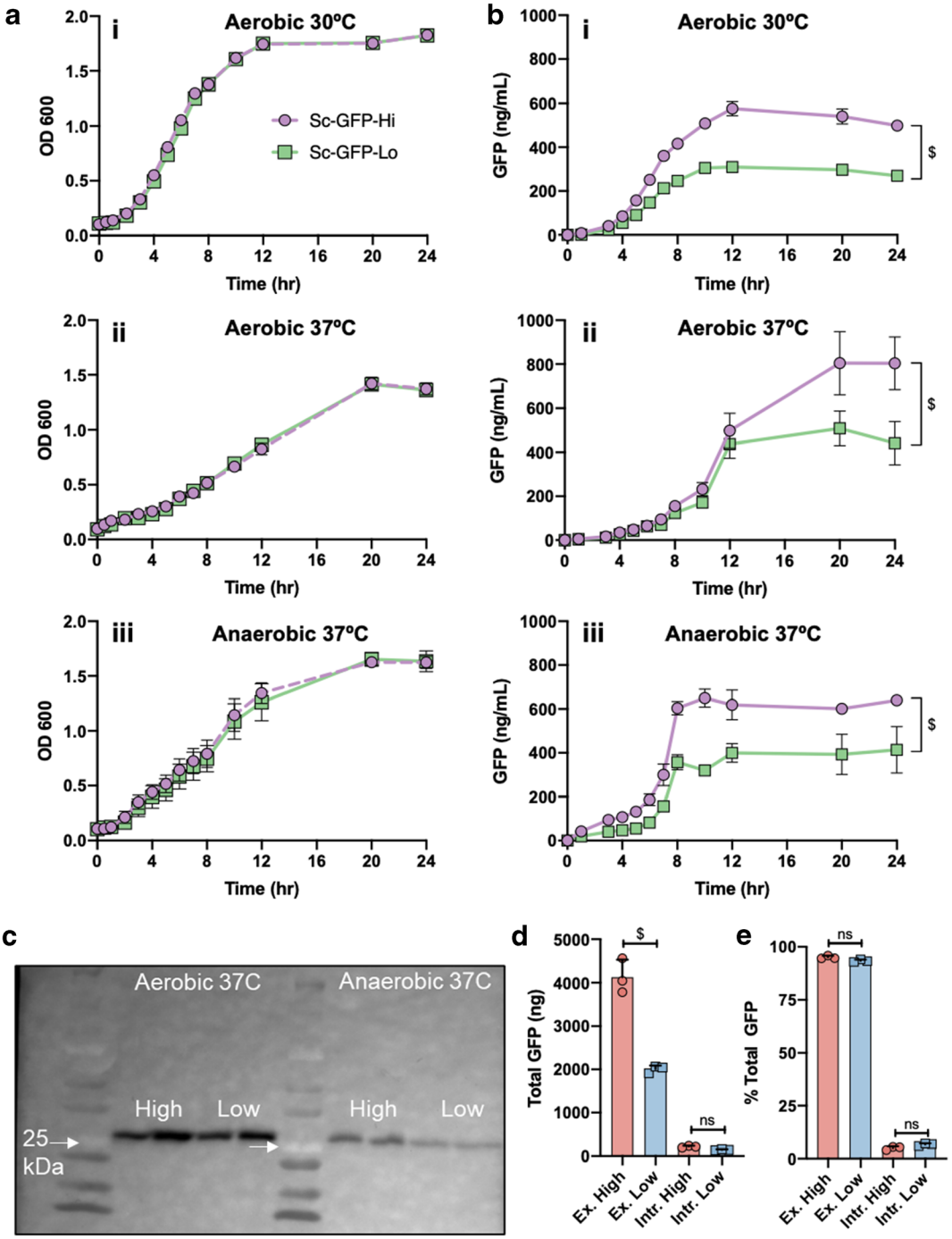

Fig. 2. Growth and GFP secretion under various conditions. **a** Growth curves for Sc-GFP-Hi and Sc-GFP-Lo under (i) aerobic conditions at 30°C, (ii) aerobic conditions at 37°C, and (iii) anaerobic conditions at 37°C. **b** GFP concentrations for Sc-GFP-Hi and Sc-GFP-Lo under (i) aerobic conditions at 30°C, (ii) aerobic conditions at 37°C, and (iii) anaerobic conditions at 37°C. **c** Western blot analysis of culture supernatants (n=2 biological replicates). **d** Analysis of total extracellular (Ex.) and intracellular (Intr.) GFP from Sc-GFP-Hi and Sc-GFP-Lo cultures under aerobic conditions at 37°C. **e** Percent intracellular and extracellular GFP from Sc-GFP-Hi and Sc-GFP-Lo cultures. For **a**, **b**, **d**, and **e**, each point represents the mean of n=3 biological replicates, error bars represent standard deviation, significance assessed using unpaired Student's t-test, $: $p < 0.0001$

decreased GFP detection associated with a lower initial dose (Fig. 4f); linear representation of the GFP concentrations in the GI tissues demonstrated the same trend (Fig. S5). Finally, GFP was not detected in the small intestines of 24/25 of the mice, likely due to the extensive protein degradation that occurs in the small intestine (57).

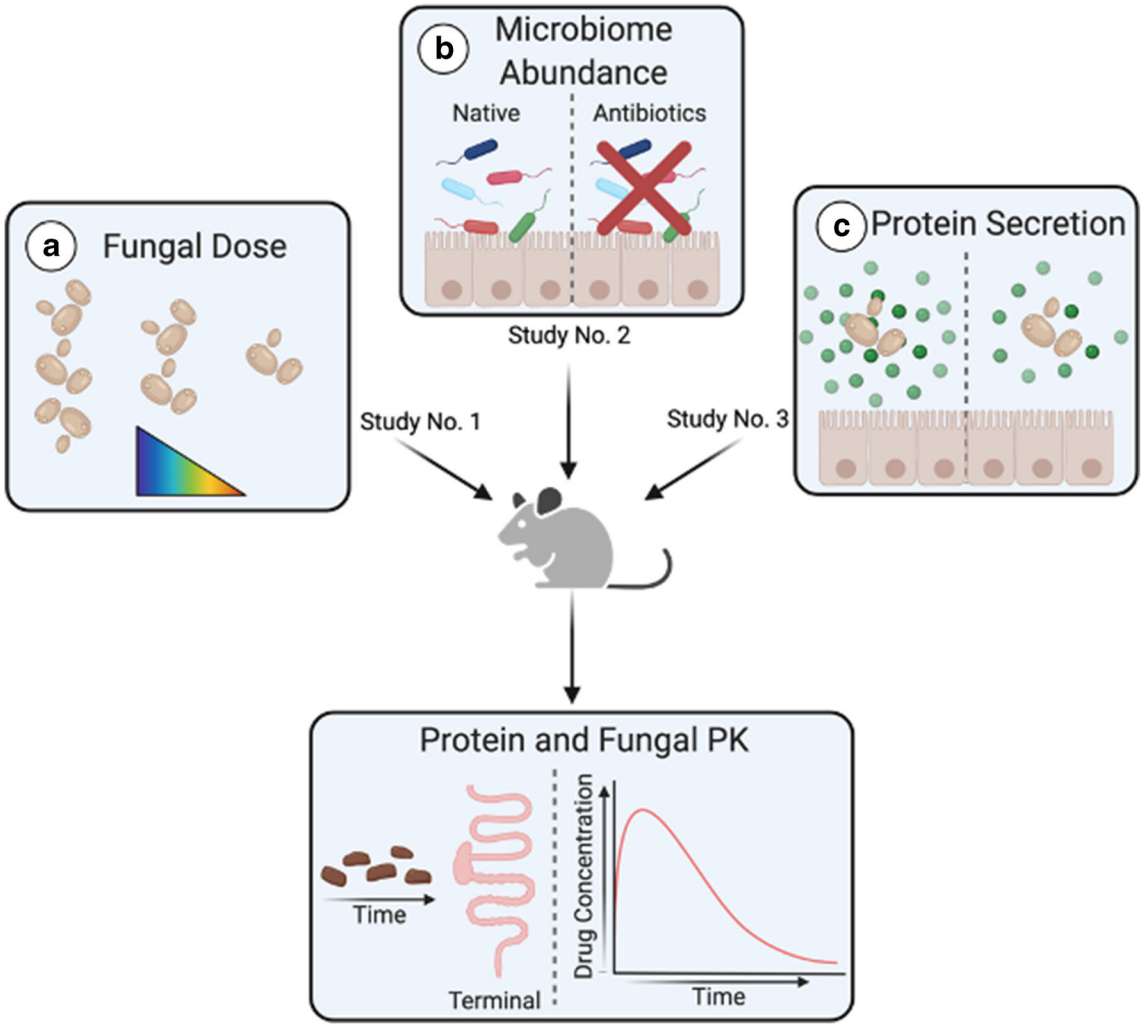

Fig. 3. Schematic of animal experiments. Schematic of investigated approaches, and measured outputs, for modulating the *in vivo* pharmacokinetics of engineered fungi and secreted GFP. These approaches include **a** altering oral dose of engineered fungi, **b** co-administering antibiotics, and **c** altering recombinant protein secretion titer.

Controlling Total Engineered Fungal and GFP Exposures in Mice by Modulating the Microbial Abundance of the Native Microbiome

Previous literature suggests that the presence of native microbes in the GI microbiome can prevent the long-term persistence or the establishment of a niche for stable colonization of exogenously administered microbes (58,59). We observed this in our preliminary studies, where we showed that in the absence of antibiotic pre-treatment or co-administration, the engineered fungi were cleared from the GI tract within 48 h of oral administration (Fig. S6). To overcome this colonization resistance due to the native microbiome, antibiotics are frequently used as a pre-treatment to the administration of fecal microbiota transplants and/or other microbial consortia to promote colonization of the exogenous microbes (60–62). Thus, we sought to understand the relationship between native microbial abundance with both engineered fungal persistence in the GI tract and with the GI pharmacokinetics of GFP.

To modulate native microbial abundance, we exposed mice to antibiotics for 3 days prior to oral gavage of Sc-GFP-Hi and throughout the duration of the study (pre-plus continuous antibiotics), only 3 days prior to oral gavage of Sc-GFP-Hi (pre-antibiotics), or no antibiotics (Fig. 5a). The mice that received the pre-plus continuous antibiotics treatment showed a persistent concentration of CFUs around 10^7 CFU g^{-1} in the feces over 1 week (Fig. 5b). This is consistent with the previous reports of fungal administration to antibiotic-treated mice (43,44). Mice which received only the pre-antibiotic treatment showed a peak concentration of about 10^8 CFU g^{-1} in the feces at 6 h post-gavage which decreased over the first 3 days and then tapered out to a stable concentration of around 10^3 CFU g^{-1} in the feces for the remainder of the week (Fig. 5b). Mice which received no antibiotics showed a peak concentration of about 10^7 CFU g^{-1} in the feces at 6 h post-gavage which mostly cleared within 24 h post-gavage, suggesting a transient passage and clearance of Sc-GFP-Hi (Fig. 5b) which is consistent with our preliminary results and previous literature (56). An area under the curve (AUC) analysis demonstrated that the AUCs were significantly different between each of the groups, with the pre-plus continuous antibiotic group having the highest

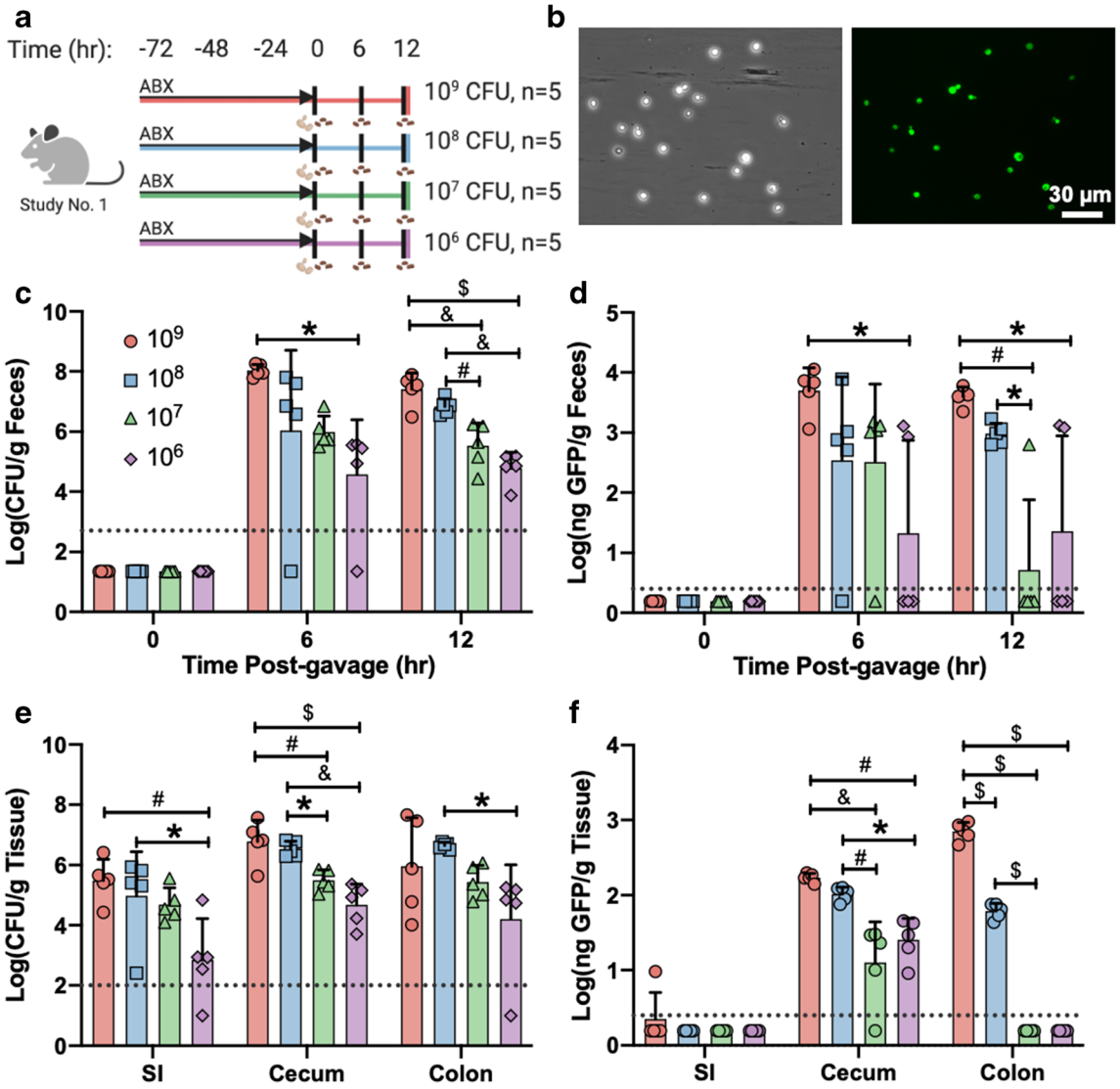

Fig. 4. Influence of dose on engineered fungal and GFP pharmacokinetics. **a** Timeline of animal study for evaluating oral dose. Yellow dots indicate oral gavage of engineered fungi, brown dots indicate fecal collection time points, and black arrows indicate antibiotic administration. **b** Representative brightfield and fluorescence microscopy images of engineered fungi isolated from fecal samples. **c** Fecal CFUs of Sc-GFP-Hi per gram of feces. **d** Fecal GFP concentrations, on a per gram of feces basis. **e** CFU concentrations in small intestine (SI), cecum, and colon of mice 12 h post-gavage. **f** GFP concentrations in SI, cecum, and colon of mice 12 h post-gavage. All error bars represent standard deviation, significance assessed using ordinary one-way ANOVA with multiple comparisons, n=5 for all panels. Horizontal dotted lines represent the limit of detection for each specific assay. For all statistical tests, $^{*}p < 0.05$, $^{\#}p < 0.01$, $^{\&}p < 0.001$, and $^{\$}p < 0.0001$

AUC, followed by the pre-antibiotic, and then the no antibiotic group (Fig. 5c). Similar GFP concentration profiles were observed in the feces where the mice continuously treated with antibiotics exhibited consistent GFP fecal concentrations, mice treated with only the antibiotic pre-treatment showed high fecal concentrations of GFP at early time points followed by a decline, and the mice receiving no antibiotics showed GFP signal in feces only within the first 48 h post-gavage (Fig. 5d). An AUC analysis of fecal GFP showed that the GI persistence of the engineered microbe, as modulated by antibiotic administration, significantly alters the concentration of the secreted GFP in the feces over the course of 1 week (Fig. 5e).

An analysis of the local tissue concentrations of both Sc-GFP-Hi and GFP within the GI tract 7 days post-gavage revealed the presence of CFU and recombinant GFP primarily in the group which received pre-plus continuous antibiotics (Fig. 5f and g). Although all five mice in the antibiotics pre-treatment group showed CFUs in the feces on day 7, CFUs were detected in the small intestine of only one mouse of in this group, and GFP was detected in the cecum of two mice in this group. Both CFUs and GFP were undetected in any part of the GI tract on day 7 in the mice which did not receive antibiotics. A linear representation of the GFP concentrations in the GI tissues demonstrated the same trends (Fig. S7) as the log representation (Fig. 5g).

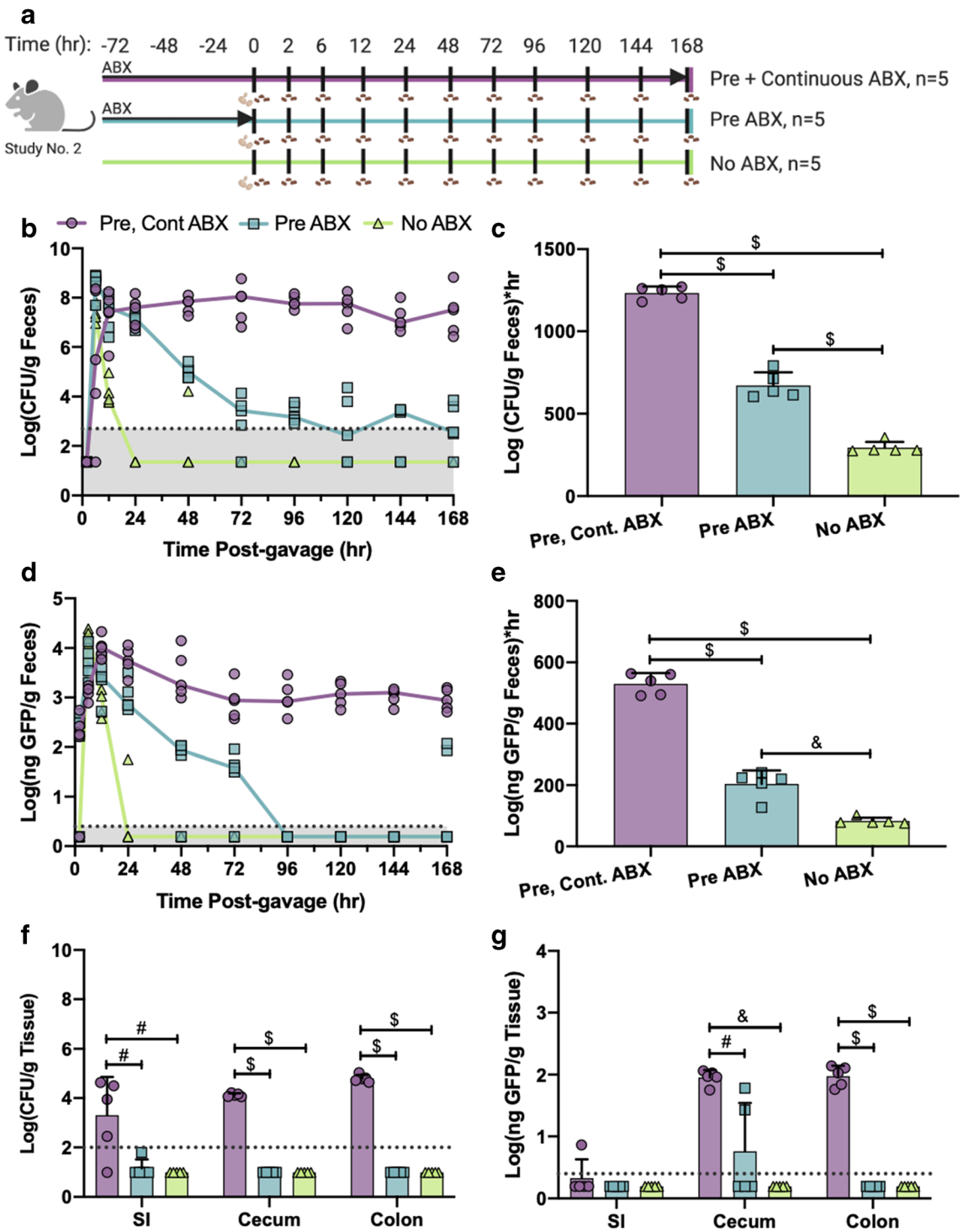

Fig. 5. Influence of native microbial abundance on engineered fungal and GFP pharmacokinetics. **a** Timeline of animal study to evaluate role of antibiotics. Yellow dots indicate oral gavage of engineered fungi, brown dots indicate fecal collection time points, and black arrows indicate antibiotic administration. **b** Fecal CFUs of Sc-GFP-Hi over a period of 1 week. **c** AUC analysis of fecal CFUs. **d** Fecal GFP concentrations over 1 week. **e** AUC analysis of fecal GFP. **f** CFU in small intestine (SI), cecum, and colon of mice 1 week post-gavage. **g** GFP concentrations in SI, cecum, and colon of mice 1 week post-gavage. All error bars represent standard deviation, significance assessed using ordinary one-way ANOVA with multiple comparisons, n=5 for all panels. For **b** and **d**, lines represent median. Horizontal dotted lines represent the limit of detection for each specific assay. For all statistical tests, $^{\#}p < 0.01$, $^{\&}p < 0.001$, and $^{\$}p < 0.0001$

Influence of Secretion Titer on Local Gastrointestinal Concentrations of Engineered Fungi and Secreted GFP in Mice

Here, we studied the effect that protein secretion had on both engineered fungal and GFP concentrations in the feces and local tissues in mice after receiving the same oral dose of either Sc-GFP-Hi or Sc-GFP-Lo (Fig. 6a). Both groups received pre-plus continuous antibiotics to enable stable colonization of the engineered fungi. An analysis of the CFU in the feces over the course of 1 week showed a constant concentration of approximately 10^7 CFU g^{-1} feces, for both groups (Fig. 6b). There were no statistical differences between the two groups with regard to CFU in the feces, indicating that the *in vitro* protein secretion titer differences did not alter the *in vivo* engineered fungal pharmacokinetics. There were no statistical differences between the two groups for the concentration of GFP in the feces over the course of the week (Fig. 6c). Animals that received Sc-GFP-Lo showed higher (but not statistically significant) CFU concentrations within the GI tissues as compared to Sc-GFP-Hi (Fig. 6d). Despite this, the group which received Sc-GFP-Hi showed significantly higher GFP concentrations within the cecum and colon (Fig. 6e). As with the two previous animal experiments, the linear representation of the GFP concentrations in the GI tissues demonstrated the same trend (Fig. S8) as the log representation (Fig. 6e). To evaluate the long-term effects of the engineered fungi on the mice, we measured their weights throughout the entirety of the study (Fig. 6f) which showed that administration of the engineered fungi did not cause any significant weight loss compared to control groups.

DISCUSSION

Overall, this work demonstrates a thorough analysis of concentration versus time profiles for an engineered, recombinant protein-secreting fungus, ultimately elucidating several approaches for modulating the pharmacokinetics and local concentrations of both the engineered fungi and its secreted

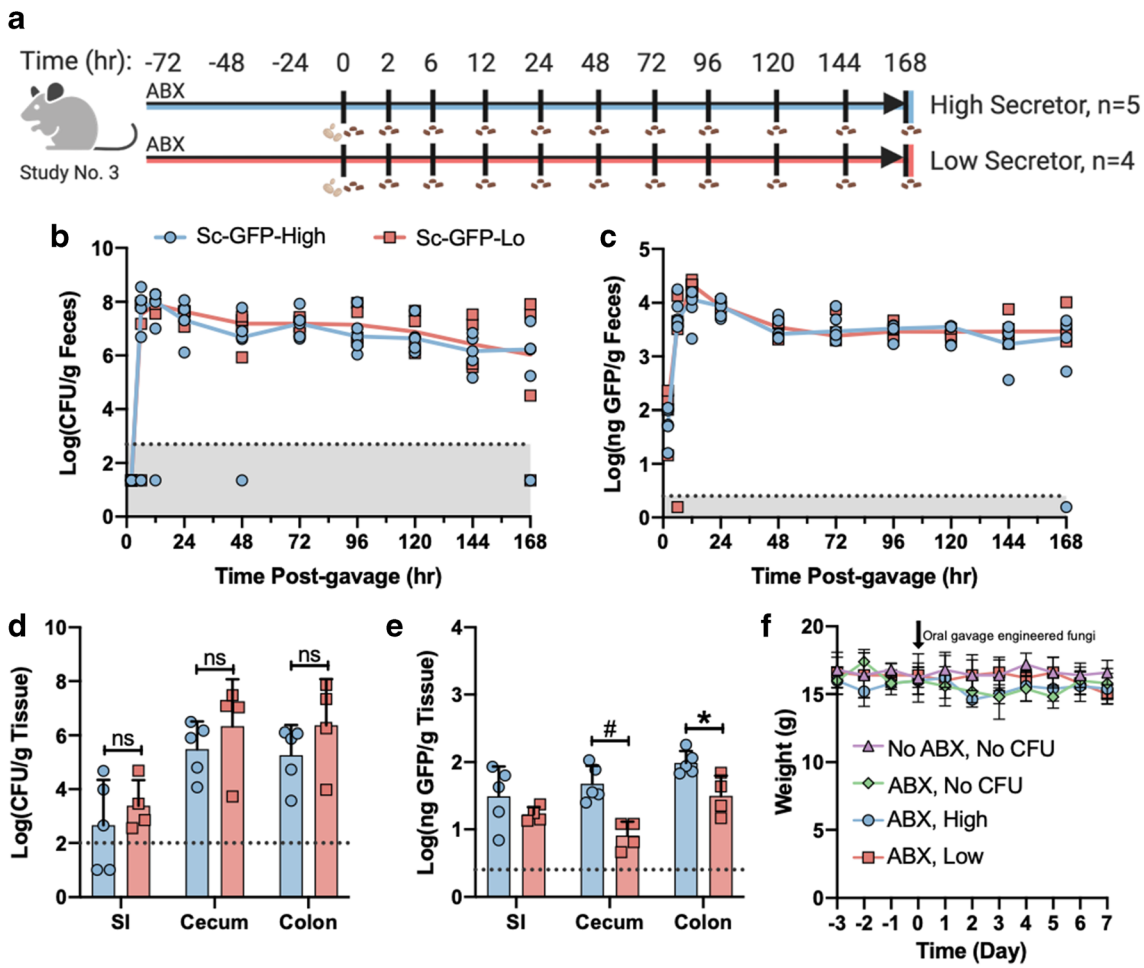

Fig. 6. Influence of *in vitro* secretion titer on *in vivo* engineered fungal and GFP pharmacokinetics. **a** Timeline of animal study to evaluate role of secretion titer. Yellow dots indicate oral gavage of engineered fungi, brown dots indicate fecal collection time points, and black arrows indicate antibiotic administration. **b** Fecal CFUs of Sc-GFP-Hi and Sc-GFP-Lo over 1 week. **c** Fecal GFP concentrations of Sc-GFP-Hi and Sc-GFP-Lo over 1 week. **d** CFU in small intestine (SI), cecum, and colon of mice 1 week post-gavage. **e** GFP concentrations in SI, cecum, and colon of mice 1 week post-gavage. **f** Mouse weights over the course of the study. All error bars represent standard deviation, significance assessed using ordinary one-way ANOVA with multiple comparisons, n=4 (Sc-GFP-Lo) or 5 (Sc-GFP-Hi). For **b** and **c**, lines represent median. Horizontal dotted lines represent the limit of detection for each specific assay. For all statistical tests, $^{*}p < 0.05$, $^{\#}p < 0.01$

recombinant protein. We showed that a *Saccharomyces cerevisiae* engineered to secrete a complex protein such as GFP was able to grow under a variety of conditions representative of those in the GI tract (36,50). We characterized the *in vitro* secretion profiles of differentially expressing engineered isolates as a means to control the *in vivo* GFP delivery (Fig. 2). Here, we present three approaches to modulate the *in vivo* pharmacokinetics of an engineered fungi drug delivery system through (i) altering oral dose of engineered fungi (Fig. 3a), (ii) co-administering antibiotics (Fig. 3b), and (iii) altering recombinant protein secretion titer (Fig. 3c).

First, we studied how dose affected the local GI concentrations of both the engineered fungi and secreted GFP using Sc-GFP-Hi (Fig. 4). Generally, and as expected, higher doses correlated with higher CFU counts and GFP signal in both the feces and GI tissues (cecum and colon). We then studied how antibiotics, which decrease the abundance of endogenous bacteria in the GI tract, altered the fungal and GFP exposures in mice (Fig. 5). In this experiment, we showed that antibiotic co-administration can prolong the GI persistence of the engineered fungi and thus GFP exposure over a period of 1 week. Our results also highlight that a consistent exposure to the engineered fungi will result in constant secretion and subsequent delivery of the secreted recombinant protein; in contrast, clearance of the engineered fungi will lead to loss of GFP persistence in the GI tract. This experiment also supports the hypothesis that the presence of native bacteria prevents the colonization of engineered fungi, possibly through means of lack of physical space and competition for nutrients (59). Finally, we studied the effect that secretion titer, through direct comparison between Sc-GFP-Hi and Sc-GFP-Low, has on fungal persistence and GFP concentration in the GI tract (Fig. 6). In this experiment, we saw that higher secretion titer did not affect fungal persistence; however, as expected, GFP concentrations in the cecum and colon were higher for Sc-GFP-Hi. This validated the notion that a microbe which secretes a higher amount of the recombinant protein *in vitro* can deliver higher amounts of recombinant protein *in vivo*. Overall, our *in vivo* experiments demonstrated that oral dose, antibiotic exposure, and secretion titer of the engineered fungi all play key roles in the local delivery of a recombinant protein from engineered LBPs.

Importantly, the approaches described here can be applied to study the oral delivery of complex proteins or peptides via LBPs to establish time-dependent, pharmacokinetic-pharmacodynamic relationships. To our knowledge, this is the first study to report that modulation of microbial dose or secretion titer directly influences delivered recombinant protein concentrations in the GI tract in as little as 12 h. Modulation of oral dose and/or protein secretion titers can aid in determining potentially non-linear dose-response relationships in pre-clinical development and can be used in clinical practice to fine-tune the dosing regimen. Altogether these results represent a step forward in the potential for optimized pre-clinical development and clinical translation of LBPs. With predictable and tunable kinetics, the translation of these platforms to therapeutic applications can potentially be optimized to control local concentrations of the secreted therapeutic.

As with the exploration of any model system, there are limitations to the translatability of these results. Most evidently, the secretion of a protein other than GFP from an engineered fungus will have its own intrinsic transport profiles, degradation rates, and clearance mechanisms which will dictate the resulting pharmacokinetics (63,64). Additionally, the detection of the secreted protein in tissue samples may be dependent on the time of sample collection as activities such as peristalsis, food intake, and secretion of protein-degrading enzymes into the distinct sections of the small intestine (i.e., duodenum, jejunum, and ileum) are dynamic and vary throughout the day in mice (65,66). For example, these variables may have contributed to the discrepancies observed in the ability to detect GFP in the small intestine in the first and second *in vivo* studies (Figs. 4f and 5g), as compared to the third *in vivo* study (Fig. 6e). Future studies are needed to evaluate the effect of tissue collection time for the distinct small intestine sections (i.e., duodenum, jejunum, ileum) on the detection and quantification of the secreted proteins. Furthermore, we hypothesize in the first *in vivo* study (Fig. 4f) that GFP concentrations for the lower doses (10^7 and 10^6 CFU) were undetectable in the colon because tissue samples were collected 12 h post-administration, leaving less time for the engineered fungi to acclimate, proliferate, and secrete GFP that would provide detectable levels; we additionally posit that the higher doses (10^9 and 10^8 CFU), which provided high GFP concentrations in the colon, were less affected by these factors due to their significantly higher concentration both initially and throughout the duration of the study (Fig. 4d).

Separately, although the practice of measuring microbial abundances in the feces as a proxy for GI concentrations is well-established (67,68), such methods are not established for recombinant proteins secreted by proliferating LBPs in the GI tract. The concentrations of GFP, or any other microbe-secreted recombinant protein, in the feces certainly captures the past presence (or lack thereof) of the protein in the GI tract. However, these measurements may not be accurately representative of protein concentrations within specific sections of the GI tract and do not represent the (often non-linear) spatiotemporal dynamics of protein diffusion, degradation, absorption, and clearance (31,69,70). We hypothesize that significant differences in GFP concentrations in the feces were not detected between the two groups in the third *in vivo* study (Fig. 6c) due to non-linear clearance and non-linear metabolism/degradation pathways which the secreted GFP experienced as it passed through the GI tract or was excreted into the fecal pellet (71–73). The *in vitro* differential GFP secretion between these two strains was approximately 2-fold in saturated cultures. Potentially 10-, 100- or even greater fold *in vitro* secretion differences may be needed to overcome non-linear processes in the GI tract to be able to detect statistical differences in fecal pellet protein concentrations. Thus, although the feces may capture general pharmacokinetic trends, measurements made in the specific sections of the GI tract are, in our opinion, more important for establishing dose-response relationships in future applications of LBPs targeting the GI tract. These site-specific measurements will directly quantify recombinant protein concentrations at the site of action. Thus, fecal protein concentration measurements should be taken with caution and an

understanding of underlying mechanisms occurring within the GI tract which may confound exact protein concentrations in fecal pellets.

Future work will be focused on translating this platform to various therapeutic applications. The next important step after establishing predictable pharmacokinetics would be to relate the pharmacokinetic profiles to the pharmacodynamic response profiles. Because of the mature and well-validated protein secretion and genetic engineering strategies already developed for *S. cerevisiae,* there is much potential for the oral delivery of a wide variety of therapeutic, immune-stimulating, anti-microbial, etc. proteins targeted directly to the GI tract. For example, an anti-microbial peptide to target the killing of specific bacteria in the GI tract could be delivered or therapeutic proteins could be delivered to specific sites of inflammation in the GI tract for treatment of ulcerative colitis or colorectal cancer. Furthermore, this platform could be used to deliver immune stimulating proteins for mucosal vaccination for the development of oral vaccines.

CONCLUSIONS

Importantly, here we establish the fundamental pharmacokinetics which will inform the downstream pharmacodynamic response regardless of the specific recombinant protein delivered. Collectively, this manuscript provides several methods for modulating engineered fungal GI pharmacokinetics which will be essential when studying future mechanisms of action and establishing dose-response relationships in future therapeutic applications of this system. This sets the groundwork for being able to specifically tune the effective dose and subsequent response to the LBP in a therapeutic model. Broadly, this work contributes to the progression of precision-based, microbiome therapeutics which have only just begun to show their potential. There is also potential for the secretion of multiple different proteins from a single engineered microbial strain in addition to the potential for the oral delivery of a cocktail of multiple microbial strains with varying functions for combination therapies.

SUPPLEMENTARY INFORMATION

The online version contains supplementary material available at https://doi.org/10.1208/s12248-021-00606-9.

ACKNOWLEDGEMENTS

We thank Dr. J. Heitman for kindly gifting the wild type fungal strain. We thank UNC Nanomedicines Characterization Core Facility for training and equipment utilization for western blot imaging. Illustrations created with BioRender.com.

AUTHOR CONTRIBUTION

M.H. and A.A. conceived the ideas presented, designed the studies, organized experimental work, and wrote and revised the manuscript. M.H. performed all experiments and data analyses. A.A. supervised the project and data analyses. M.H. and A.A agree to be accountable for all aspects of the work in ensuring that questions related to the accuracy or integrity of any part of the work are appropriately investigated and resolved.

FUNDING

Research reported in this publication was supported by the National Institute of General Medical Sciences of the National Institutes of Health under Award Number R35GM137898.

DECLARATIONS

Conflict of interest The authors declare no competing interests.

Disclaimer The content is solely the responsibility of the authors and does not necessarily represent the official views of the National Institutes of Health.

Data statement All data needed to evaluate the conclusions in the paper are present in the paper and/or the Supplementary Information. Additional data related to this paper may be requested from the authors.

REFERENCES

1. Human Microbiome Project C. Structure, function and diversity of the healthy human microbiome. Nature. 2012;486(7402):207–14.
2. Belkaid Y, Hand TW. Role of the microbiota in immunity and inflammation. Cell. 2014;157(1):121–41.
3. Cho I, Blaser MJ. The human microbiome: at the interface of health and disease. Nat Rev Genet. 2012;13(4):260–70.
4. Yatsunenko T, Rey FE, Manary MJ, Trehan I, Dominguez-Bello MG, Contreras M, et al. Human gut microbiome viewed across age and geography. Nature. 2012;486(7402):222–7.
5. Nkamga VD, Henrissat B, Drancourt M. Archaea: essential inhabitants of the human digestive microbiota. Hum Microb J. 2017;3:1–8.
6. Underhill DM, Iliev ID. The mycobiota: interactions between commensal fungi and the host immune system. Nat Rev Immunol. 2014;14(6):405–16.
7. Subramanian S, Blanton LV, Frese SA, Charbonneau M, Mills DA, Gordon JI. Cultivating healthy growth and nutrition through the gut microbiota. Cell. 2015;161(1):36–48.
8. Lukes J, Stensvold CR, Jirku-Pomajbikova K, Wegener PL. Are human intestinal eukaryotes beneficial or commensals? PLoS Pathog. 2015;11(8):e1005039.
9. Fischbach MA, Sonnenburg JL. Eating for two: how metabolism establishes interspecies interactions in the gut. Cell Host Microbe. 2011;10(4):336–47.
10. Cerf-Bensussan N, Gaboriau-Routhiau V. The immune system and the gut microbiota: friends or foes? Nat Rev Immunol. 2010;10(10):735–44.
11. Zuo T, Ng SC. The gut microbiota in the pathogenesis and therapeutics of inflammatory bowel disease. Front Microbiol. 2018;9:2247.
12. Louis P, Hold GL, Flint HJ. The gut microbiota, bacterial metabolites and colorectal cancer. Nat Rev Microbiol. 2014;12(10):661–72.
13. Sampson TR, Debelius JW, Thron T, Janssen S, Shastri GG, Ilhan ZE, et al. Gut microbiota regulate motor deficits and neuroinflammation in a model of parkinson's disease. Cell. 2016;167(6):1469–80 e12.

14. Riglar DT, Silver PA. Engineering bacteria for diagnostic and therapeutic applications. Nat Rev Microbiol. 2018;16(4):214–25.
15. Charbonneau MR, Isabella VM, Li N, Kurtz CB. Developing a new class of engineered live bacterial therapeutics to treat human diseases. Nat Commun. 2020;11(1):1738.
16. Claesen J, Fischbach MA. Synthetic microbes as drug delivery systems. ACS Synth Biol. 2015;4(4):358–64.
17. Isabella VM, Ha BN, Castillo MJ, Lubkowicz DJ, Rowe SE, Millet YA, et al. Development of a synthetic live bacterial therapeutic for the human metabolic disease phenylketonuria. Nat Biotechnol. 2018;36(9):857–64.
18. Daeffler KN, Galley JD, Sheth RU, Ortiz-Velez LC, Bibb CO, Shroyer NF, et al. Engineering bacterial thiosulfate and tetrathionate sensors for detecting gut inflammation. Mol Syst Biol. 2017;13(4):923.
19. Leventhal DS, Sokolovska A, Li N, Plescia C, Kolodziej SA, Gallant CW, et al. Immunotherapy with engineered bacteria by targeting the STING pathway for anti-tumor immunity. Nat Commun. 2020;11(1):2739.
20. Steidler L, Hans W, Schotte L, Neirynck S, Obermeier F, Falk W, et al. Treatment of murine colitis by Lactococcus lactis secreting interleukin-10. Science. 2000;289(5483):1352–5.
21. Durmusoglu D, Al'Abri IS, Collins SP, Cheng J, Eroglu A, Beisel CL, et al. In situ biomanufacturing of small molecules in the mammalian gut by probiotic saccharomyces boulardii. ACS Synth Biol. 2021.
22. Brown TD, Whitehead KA, Mitragotri S. Materials for oral delivery of proteins and peptides. Nat Rev Mater. 2019;5(2):127–48.
23. Anselmo AC, Gokarn Y, Mitragotri S. Non-invasive delivery strategies for biologics. Nat Rev Drug Discov. 2019;18(1):19–40.
24. Vargason AM, Anselmo AC. Clinical translation of microbe-based therapies: current clinical landscape and preclinical outlook. Bioeng Transl Med. 2018;3(2):124–37.
25. Wang LLW, Janes ME, Kumbhojkar N, Kapate N, Clegg JR, Prakash S, *et al*. Cell therapies in the clinic. Bioeng Transl Med. 2021;n/a(n/a):e10214.
26. Rowland M, Peck C, Tucker G. Physiologically-based pharmacokinetics in drug development and regulatory science. Annu Rev Pharmacol Toxicol. 2011;51:45–73.
27. Shah DK, Betts AM. Towards a platform PBPK model to characterize the plasma and tissue disposition of monoclonal antibodies in preclinical species and human. J Pharmacokinet Pharmacodyn. 2012;39(1):67–86.
28. Gobeau N, Stringer R, De Buck S, Tuntland T, Faller B. Evaluation of the GastroPlus Advanced Compartmental and Transit (ACAT) Model in Early Discovery. Pharm Res. 2016;33(9):2126–39.
29. Jimenez M, Langer R, Traverso G. Microbial therapeutics: new opportunities for drug delivery. J Exp Med. 2019;216(5):1005–9.
30. Eisenstein M. The hunt for a healthy microbiome. Nature. 2020;577(7792):S6–8.
31. Lichtman JS, Sonnenburg JL, Elias JE. Monitoring host responses to the gut microbiota. ISME J. 2015;9(9):1908–15.
32. Zhang S, Ermann J, Succi MD, Zhou A, Hamilton MJ, Cao B, et al. An inflammation-targeting hydrogel for local drug delivery in inflammatory bowel disease. Sci Transl Med. 2015;7(300):300ra128.
33. Xie YH, Chen YX, Fang JY. Comprehensive review of targeted therapy for colorectal cancer. Sign Transduct Target Ther. 2020;5(1):22.
34. Huang M, Bao J, Hallstrom BM, Petranovic D, Nielsen J. Efficient protein production by yeast requires global tuning of metabolism. Nat Commun. 2017;8(1):1131.
35. Costenoble R, Adler L, Niklasson C, Liden G. Engineering of the metabolism of Saccharomyces cerevisiae for anaerobic production of mannitol. FEMS Yeast Res. 2003;3(1):17–25.
36. Espey MG. Role of oxygen gradients in shaping redox relationships between the human intestine and its microbiota. Free Radic Biol Med. 2013;55:130–40.
37. Jeong H, Arif B, Caetano-Anolles G, Kim KM, Nasir A. Horizontal gene transfer in human-associated microorganisms inferred by phylogenetic reconstruction and reconciliation. Sci Rep. 2019;9(1):5953.
38. Lerner A, Matthias T, Aminov R. Potential effects of horizontal gene exchange in the human gut. Front Immunol. 2017;8:1630.
39. Fitzgerald I, Glick BS. Secretion of a foreign protein from budding yeasts is enhanced by cotranslational translocation and by suppression of vacuolar targeting. Microb Cell Factories. 2014;13(1):125.
40. Dolinski K, Muir S, Cardenas M, Heitman J. All cyclophilins and FK506 binding proteins are, individually and collectively, dispensable for viability in Saccharomyces cerevisiae. Proc Natl Acad Sci U S A. 1997;94(24):13093–8.
41. Chao G, Lau WL, Hackel BJ, Sazinsky SL, Lippow SM, Wittrup KD. Isolating and engineering human antibodies using yeast surface display. Nat Protoc. 2006;1(2):755–68.
42. Gietz RD, Schiestl RH. High-efficiency yeast transformation using the LiAc/SS carrier DNA/PEG method. Nat Protoc. 2007;2(1):31–4.
43. Jiang TT, Shao TY, Ang WXG, Kinder JM, Turner LH, Pham G, et al. Commensal fungi recapitulate the protective benefits of intestinal bacteria. Cell Host Microbe. 2017;22(6):809–16 e4.
44. Jiang TT, Chaturvedi V, Ertelt JM, Xin L, Clark DR, Kinder JM, et al. Commensal enteric bacteria lipopolysaccharide impairs host defense against disseminated Candida albicans fungal infection. Mucosal Immunol. 2015;8(4):886–95.
45. Bzducha-Wrobel A, Blazejak S, Kawarska A, Stasiak-Rozanska L, Gientka I, Majewska E. Evaluation of the efficiency of different disruption methods on yeast cell wall preparation for beta-glucan isolation. Molecules. 2014;19(12):20941–61.
46. Plessis A, Dujon B. Multiple tandem integrations of transforming DNA sequences in yeast chromosomes suggest a mechanism for integrative transformation by homologous recombination. Gene. 1993;134(1):41–50.
47. Casler JC, Glick BS. Visualizing secretory cargo transport in budding yeast. Curr Protoc Cell Biol. 2019;83(1):e80.
48. Verstrepen KJ, Jansen A, Lewitter F, Fink GR. Intragenic tandem repeats generate functional variability. Nat Genet. 2005;37(9):986–90.
49. Evanko D. Training GFP to fold. Nat Methods. 2006;3(2):76.
50. Zheng L, Kelly CJ, Colgan SP. Physiologic hypoxia and oxygen homeostasis in the healthy intestine. A review in the theme: cellular responses to hypoxia. Am J Phys Cell Physiol. 2015;309(6):C350–60.
51. Munna MS, Humayun S, Noor R. Influence of heat shock and osmotic stresses on the growth and viability of Saccharomyces cerevisiae SUBSC01. BMC Res Notes. 2015;8(1):369.
52. Pizarro FJ, Jewett MC, Nielsen J, Agosin E. Growth temperature exerts differential physiological and transcriptional responses in laboratory and wine strains of Saccharomyces cerevisiae. Appl Environ Microbiol. 2008;74(20):6358–68.
53. Prasher DC, Eckenrode VK, Ward WW, Prendergast FG, Cormier MJ. Primary structure of the Aequorea victoria green-fluorescent protein. Gene. 1992;111(2):229–33.
54. Garber K. First microbiome-based drug clears phase III, in clinical trial turnaround. Nat Rev Drug Discov. 2020;19(10):655–6.
55. Cordaillat-Simmons M, Rouanet A, Pot B. Live biotherapeutic products: the importance of a defined regulatory framework. Exp Mol Med. 2020;52(9):1397–406.
56. Auchtung TA, Fofanova TY, Stewart CJ, Nash AK, Wong MC, Gesell JR, et al. Investigating colonization of the healthy adult gastrointestinal tract by fungi. mSphere. 2018;3(2):e00092–18.
57. Arike L, Seiman A, van der Post S, Rodriguez Pineiro AM, Ermund A, Schutte A, et al. Protein turnover in epithelial cells and mucus along the gastrointestinal tract is coordinated by the spatial location and microbiota. Cell Rep. 2020;30(4):1077–87 e3.
58. Sorbara MT, Pamer EG. Interbacterial mechanisms of colonization resistance and the strategies pathogens use to overcome them. Mucosal Immunol. 2019;12(1):1–9.
59. Ducarmon QR, Zwittink RD, Hornung BVH, van Schaik W, Young VB, Kuijper EJ. Gut microbiota and colonization resistance against bacterial enteric infection. Microbiol Mol Biol Rev. 2019;83(3):e00007–19.
60. Oliphant K, Cochrane K, Schroeter K, Daigneault MC, Yen S, Verdu EF, et al. Effects of antibiotic pretreatment of an ulcerative colitis-derived fecal microbial community on the

integration of therapeutic bacteria in vitro. mSystems. 2020;5(1):e00404–19.
61. Gopalakrishnan V, Weiner B, Ford CB, Sellman BR, Hammond SA, Freeman DJ, et al. Intervention strategies for microbial therapeutics in cancer immunotherapy. Immuno-Oncol Technol. 2020;6:9–17.
62. Schwartz DJ, Langdon AE, Dantas G. Understanding the impact of antibiotic perturbation on the human microbiome. Genome Med. 2020;12(1):82.
63. Wolfe RR, Park S, Kim IY, Starck C, Marquis BJ, Ferrando AA, et al. Quantifying the contribution of dietary protein to whole body protein kinetics: examination of the intrinsically labeled proteins method. Am J Physiol Endocrinol Metab. 2019;317(1):E74–84.
64. Di L. Strategic approaches to optimizing peptide ADME properties. AAPS J. 2015;17(1):134–43.
65. Scheving LA. Biological clocks and the digestive system. Gastroenterology. 2000;119(2):536–49.
66. Martchenko A, Martchenko SE, Biancolin AD, Brubaker PL. Circadian rhythms and the gastrointestinal tract: relationship to metabolism and gut hormones. Endocrinology. 2020;161(12).
67. Vargason AM, Santhosh S, Anselmo AC. Surface modifications for improved delivery and function of therapeutic bacteria. Small. 2020;16(25):e2001705.
68. Goodman AL, Kallstrom G, Faith JJ, Reyes A, Moore A, Dantas G, et al. Extensive personal human gut microbiota culture collections characterized and manipulated in gnotobiotic mice. Proc Natl Acad Sci U S A. 2011;108(15):6252–7.
69. Maclaren OJ, Parker A, Pin C, Carding SR, Watson AJM, Fletcher AG, et al. A hierarchical Bayesian model for understanding the spatiotemporal dynamics of the intestinal epithelium. PLoS Comput Biol. 2017;13(7):e1005688.
70. Diether NE, Willing BP. Microbial fermentation of dietary protein: an important factor in diet(-)Microbe(-)host interaction. Microorganisms. 2019;7(1).
71. Yang Y, Gunasekara M, Muhammednazaar S, Li Z, Hong H. Proteolysis mediated by the membrane-integrated ATP-dependent protease FtsH has a unique nonlinear dependence on ATP hydrolysis rates. Protein Sci. 2019;28(7):1262–75.
72. Ando H, Hisaka A, Suzuki H. A new physiologically based pharmacokinetic model for the prediction of gastrointestinal drug absorption: translocation model. Drug Metab Dispos. 2015;43(4):590–602.
73. Vaidya H, Makinde OD, Choudhari R, Prasad KV, Khan SU, Vajravelu K. Peristaltic flow of non-Newtonian fluid through an inclined complaint nonlinear tube: application to chyme transport in the gastrointestinal tract. Eur Phys J Plus. 2020;135(11):934.